http://dx.doi.org/10.5935/0103-5053.20140098

J. Braz. Chem. Soc., Vol. 25, No. 7, 1208-1217, 2014.
Printed in Brazil - ©2014 Sociedade Brasileira de Química
0103 - 5053 $6.00+0.00

Article

Complex Electrooxidation of Formic Acid on Palladium

Andressa Mota-Lima,[*,a,b] Ernesto R. Gonzalez[a] and Markus Eiswirth[b]*

[a]*Instituto de Química de São Carlos, Universidade de São Paulo, Av. Trab. São-Carlense, 400, 13560-970 São Carlos-SP, Brazil*

[b]*Fritz-Haber-Institut der Max-Planck-Gesellschaft, Faradayweg 4-6, D-14195 Berlin, Germany*

Neste trabalho, a eletrooxidação oscilatória de ácido fórmico (FA) é investigada sobre paládio policristalino e comparada a resultados obtidos sobre platina policristalina; as principais diferenças entre ambas as superfícies são atribuídas a diferentes cinéticas da sub-rede química tanto quanto a rotas preferenciais admitidas sobre a superfície de paládio. Com o intuito de presumir a taxa cinética de acumulação de veneno sobre paládio, eletrooxidação de FA foi conduzida na presença e ausência de hidrogênio dissolvido na rede cristalina do paládio. As rotas preferenciais foram presumidas a partir do padrão temporal (série temporal). Notoriamente, oscilações de potencial durante a eletrooxidação de FA possuem mínimo de potencial em 0,2 V, o que é associado a uma rápida taxa de desidrogenação direta; além disso, períodos de indução (ca. 60 min) e oscilação (20 min) estão entre os mais compridos já observados em eletroquímica, pois o hidrogênio incluso na rede cristalina do paládio reduz a taxa de acumulação de CO sobre a superfície.

Herein, oscillatory formic acid (FA) electrooxidation on polycrystalline palladium is investigated and compared with the one on polycrystalline platinum; major differences between both are attributed to differences on the kinetics of sub-set chemical network as well as to preferential routes admitted on palladium surface. To presume the kinetic rate of poison accumulation on palladium, FA oxidation was accomplished in presence of occluded hydrogen and hydrogen-free electrodes. The preferential routes were presumed from the temporal pattern. Markedly, oscillations during FA electrooxidation have minimum potential at 0.2 V, which is linked to the fast rate of direct dehydrogenation; moreover, it has one of the largest induction period (ca. 60 min) and oscillatory period (20 min) observed in electrochemistry, since subsurface hydrogen slows down the rate of CO accumulation on the surface.

Keywords: chemical kinetics, electrochemistry, electrochemical energy conversion, storage

Introduction

Complex electrooxidation involves a variety of multistable states within which autonomous oscillations are the focus of much attention. Among the interesting properties of oscillatory state, the enhanced thermodynamic efficiency[1-4] seems to be the one that would most attract the fuel-cell-technologist's attention. However, complex kinetics on palladium has been scarcely investigated. The present contribution is dedicated to analyze the complex formic acid (FA) electrooxidation on flat polycrystalline palladium and the effect of subsurface hydrogen on the oscillatory dynamic. Herein, the reader also finds a review on the major kinetic and mechanistic differences between platinum and palladium and how those differences impact the oscillatory mechanism.

Palladium electrocatalyst has economical and electrochemical advantages compared with platinum, the standard catalyst for most of the electrochemical reactions. Palladium has larger geological abundance on earth's crust and lower prices in commodity exchange. Concerning electrochemical properties, palladium's ability to promote electroreaction is attested by the hydrogen oxidation reaction (HOR) in which the exchange current (i_o) is as high as the one observed on platinum.[5] Other aspects about electrochemistry on palladium is found in reference 6.

In the 1970s, FA electrooxidation was mainly the focus of attention since FA electrooxidation is a sub-set mechanism of methanol electrooxidation. Using conventional electrochemical techniques, extensive

*e-mail: andressa@motalima.com

investigation of FA electrooxidation in acid solution was conducted on platinum[7-15] as well as on palladium.[16-20] In the 1980s, the influence of ad-atom on the kinetics of FA electrooxidation was the main target.[7-10] In the 1990s, surface spectroscopic techniques were employed to clarify the main intermediate species on the surface of palladium[16-18,20] and platinum.[13,21] In recent years, palladium gained a renewed attention motivated by its usage as a nanoparticle catalyst.

Under oscillatory regime, intriguing aspects accompany FA electrooxidation on palladium surface. Conway and co-workers[22,23] recorded potential oscillations containing spikes that extends to the maximum value of 1.6 V (*vs.* reversible hydrogen electrode, RHE) on the palladium surface, while on platinum that value is limited to 0.83 V; this dissimilarity was attributed by the author to the formation of PdO_2 at a more positive potential than 1.47 V. At this potential, the CO coverage is presumably null, thus, the authors suggest that the mechanism of positive feedback loop over the free sites is based on a chemical step of oxide reduction by the FA in the solution. On the other hand, platinum surface was extensively used to investigate physicochemical aspects toward oscillating FA electrooxidation.[24-31] Lately, oscillating spectroscopic signal belonging to intermediate species was recorded and demonstrated to be in phase with the potential.[32,33] Finally, the bifurcation theory was used to argue in favour of a non-linear dynamic driven by the electrochemical mechanism.[34,35]

The mechanism of formic acid electrooxidation on Pd and Pt follows the routes shown in Scheme 1 that was constructed based on the literature.[13,20,21,25,26,36] After FA gets adsorbed, the oxidation goes through a dual-parallel pathway. The so-called direct via (the fastest via) involves formation of weakly adsorbed (therefore, active and short living) intermediates. Formate has been identified as

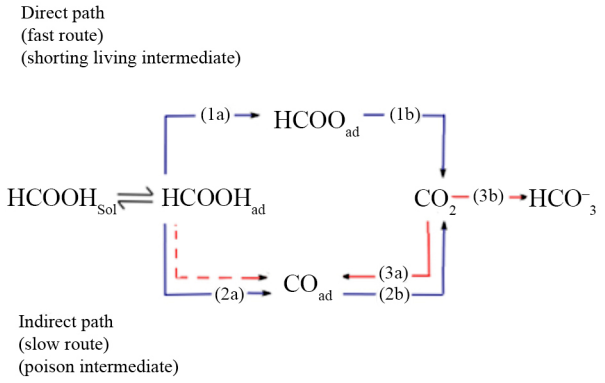

Scheme 1. Mechanism of FA oxidation on platinum (paths 1a,b and 2a,b) as well as additional mechanistic variances of FA oxidation (paths 3a,b) and suppressed routes (dotted line) observed on palladium.

fragment adsorbed on the surface in contact with formic acid in solution,[20,37] and, based on density functional theory, bridge-bonded formate was proven to be the main active intermediate;[38] formed by the following pathway:

$$HCOOH_{ads} \rightarrow HCOO_{ads} + H^+ + e^- \quad (1a)$$

And it is easily converted to CO_2 by path 1b:

$$HCOO_{ads} \rightarrow CO_2 + H^+ + e^- \quad (1b)$$

The so-called indirect via (the slowest via) involves dehydration of FA,[37,39] according to the following pathway:

$$HCOOH_{ads} \rightarrow CO_{ads} + H_2O \quad (2a)$$

and formation of strongly adsorbed intermediate, CO_{ads}, which is only oxidised at high potential (potential at which OH is formed with appreciable rate):

$$CO_{ads} + OH_{ads} \rightarrow CO_2 + H^+ + e^- \quad (2b)$$

Those two pathways operate mainly on platinum. On palladium, however, there are evidences in favour of a mechanistic variance. On Pd, FA oxidation produces CO_2 at low potential (on the hydrogen region and double layer region)[16] without detectable Fourier transform infrared spectroscopy (FTIR)-signal of adsorbed CO;[39,40] suggesting, therefore, a slower rate of CO poisoning (indirect via) on Pd than on Pt, i.e., the indirect via is suppressed on Pd (path 2a). Wang *et al.*[41] proposed that adsorbed CO has low-coverage on Pd at potentials in hydrogen region, and that derives mainly from fresh-formed CO_2 re-adsorption and reduction, path 3a, rather than deriving from FA residue. Moreover, there are stronger evidences in favour of other intermediates than simple CO or formate during FA electrooxidation on palladium. Miyake *et al.*[20] claimed the presence of bicarbonate (adsorbed on the surface with two O atoms) as an intermediate in the double layer potential region. All findings about FA electrooxidation on Pd are summarised in Scheme 1 that shows in solid red lines the additional paths and in dotted red line the suppressed path.

Palladium, unlike the rest of the electrocatalysts, is a hydrogen-absorbing electrode.[42,43] For potentials lower than 60 mV (*vs.* RHE), 70% of interstitial lattices in the palladium bulk are filled with hydrogen against only 3% for higher potential.[44,45] Thus, the volume of hydrogen absorbed in the palladium bulk must be taken into account. In fact, Yépez and Scharifker[46] observed an increased rate of formate oxidation on Pd electrode containing hydrogen in its bulk. Moreover, hydrogen-loaded palladium oxidises

a CO monolayer at more negative potentials and with formation of other products besides CO_2.[47]

Herein, the parameter phase space is experimentally exploited to recognise the sort of complex dynamic present in the mechanism of FA electrooxidation operating on Palladium. The findings are confronted with the previous oscillations observed on solid palladium electrode[22,23,48] and the main kinetic and mechanistic differences are investigated. Finally, the complex mechanistic is discussed on the basis of requirements that characterise FA mechanism as an element of the electrochemical oscillator class known as hidden negative differential resistance (HNDR).[49]

Experimental

For experiments with formic acid, palladium foil (0.5 cm^2, Degussa) was used as work electrode (WE) and platinised platinum wire as counter-electrode (CE). Reversible hydrogen electrode (RHE) was prepared with the same solution used as electrolyte in the experiment. A bubble of hydrogen is formed by applying H_2-evolution potential, and the formed H_2 gas is trapped on the vessel-top. For experiments with CO oxidation, a palladium (0.45 cm^2, unknown source) and platinum (0.32 cm^2, unknown source) wires were used as WE; platinum foil with 4 cm^2 was used as CE. Mercury/mercurous sulphate, 1 mol L^{-1} H_2SO_4, was used as RE, and its potential is a standard hydrogen electrode (SHE)-measured potential of 0.65 V. So, potentials refer to the SHE in experiments with CO-oxidation and to the RHE in experiments with formic acid oxidation.

After electrochemical experiments with formic acid, part of the palladium electrode was cut to form a sample observable by scanning electron microscopy (SEM). Local analyses of composition by energy-dispersive X-ray spectroscopy (EDS) indicated solely the signal of palladium and carbon that represented 4% of total palladium. Presumably, that carbon was some residual CO adsorbed on the surface, but CO place exchange could not be an excluded possibility.

For palladium, the electrode area was measured by integrating the current due to reduction of oxide (during the cathodic sweep of a cyclic voltammogram). Considering corrections for double layer charging, integration gives the oxide monolayer charge (Q_{OH}). The real electrode area was calculated by dividing it by Q_{OH} = 420 μC *per* real-cm^2, the charge estimated for one monolayer of adsorbed oxygen (two electrons) on 1 cm^2 of (100) plane.[50] For platinum, the electrode area was measured by integrating H-adsorption peak (during anodic sweep in between 0.15 and 0.5 V). After discounting the double layer charge, the peak area was divided by the charge associated with a monolayer of adsorbed hydrogen (Q_H = 210 μC *per* real-cm^2),[51] which is justified on the basis of predominance of the (100) plane as well as equal distribution of the three low index planes.[52] Area measurements were always carried out in carefully deoxygenated solutions.

Perchloric acid (70%, Aldrich) and sulfuric acid (98%, Merck) were used to prepare the support electrolyte while formic acid (98%, Fluka) was employed as the electroactive species. The solutions were prepared with nanopure water (18.2 MW cm, Milli-Q system) in the concentrations 0.2 mol L^{-1} for perchloric acid, 0.33 mol L^{-1} for sulfuric acid, and 0.2 mol L^{-1} for formic acid. To guarantee contamination-free solutions, all glassware, including the three-electrode cell, were cleaned chemically. The protocol includes: (*i*) twelve hours of immersion in a basic solution of potassium permanganate (aiming to oxidise the organics); (*ii*) one hour of immersion in a mixture of acid and hydrogen peroxide (aiming to remove residual permanganate); and (*iii*) abundantly rinsing glassware with nanopure water three times at least. All glassware is handled as above described right before the experiment onset.

Working and counter electrodes were conditioned according to chemical and electrochemical cleaning protocols. The first protocol, chemical cleaning, includes the electrode immersion in the same solutions mentioned above but over a limited time, around 10 minutes; in the following procedure, the electrodes were immersed several times into nanopure water (Milli-Q water) at boiling temperature, each time with renewed water. The second protocol, electrochemical cleaning, consists of reproducing the electrochemical surface by cycling the potential, between 0.4 and 1.3 V, several times in the presence of FA till reaching a stationary profile. We observed the same effects of the electrochemical cleaning reported by Capon and Parsons,[53] the electrode becomes more activated, which presumably is due to the removal of irreversible oxides.

Electrochemical investigation employed a potentiostat (Autolab/Eco-Chemie PGSTST 30) to carry out techniques such as potential and current sweeps, potentiodynamic and galvanodynamic, respectively, as well as chronopotentiometry and chronoamperometry.

Results

FA electrooxidation under controlled current: bistability

Formic acid electrooxidation is admitted to be an HNDR-oscillator;[49] therefore, it should share the same trends observed in this class,[54] such as oscillations

under current control (or just galvanostatic oscillations). Another possibility of oscillations for an HNDR would be using external resistance (between WE and RE) but that oscillatory region is not exploited here.

In electrochemistry, the technique known as chronopotentiometry fits well into that aim of identifying parameter regions where instabilities exist. Alternatively, a current sweep (or galvanodynamic) would be employed as seen in Figure 1b. Bistability, rather than oscillations, was registered in this set of experiments. It is a typical behaviour around the Sandde-Node bifurcation point that is characterised by an abrupt change between two surface states. The active state is represented by the surface at low potential, ca. 0.25 and 0.3 V for currents 0.77 and 2.06 mA real-cm^2, respectively, in Figure 1b. The inactive state is represented by the state at high potential, for instance, ca. 1.65 V for 0.77 mA real-cm^2 in Figure 1a. Note that the active state for FA electrooxidation is located in the potential at hydrogen region, i.e., smaller than 0.35 V. On the other hand, the poisoned state is located at 1.65 V. No adsorbed CO exists at this potential, but only PdO_2.[55] The inactive state has a surface poisoned by PdO_2.

For chronopotentiometries observed in Figure 1a, the smaller the applied current, the longer the active state. Smaller applied current implies that accumulation of poison is slowed down, which, in turn, leads to longer times to reach critical poisoning coverage. Equivalent arguments stand for galvanodynamic sweeps observed in Figure 1b.

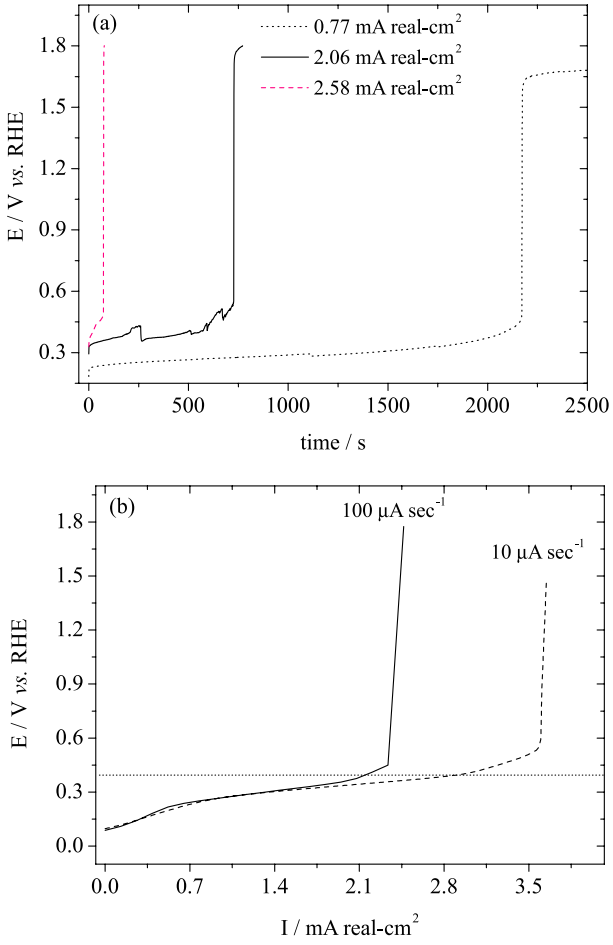

Figure 1. (a) Chronopotentiometry and (b) galvanodynamic. Experimental conditions: 0.1 mol L^{-1} H_2SO and 0.3 mol L^{-1} HCOOH; electrochemical area: 3.88 cm^2; rugosity: 7.76.

FA electrooxidation under controlled current: autonomous oscillations

Oscillations are observed at very small current, for instance, Figure 2 shows oscillations under the 0.25 mA real-cm^{-2} current density. Oscillations during FA electrooxidation are observed after 60 min, which means a large induction period (time before first spike). The same reaction on platinum[24] has less than one third of palladium induction time, i.e., less than 15 min. However, that is not the unique difference between Pd and Pt toward complex FA electrooxidation; oscillator amplitude and period also is dissimilar on both surfaces. Oscillation amplitude indicates a difference of electrical potential between two unstable states, the poisoned surface and the poison-free surface. Those states are represented by characteristic electrical potential of surface covered by underpotential deposition (UPD) hydrogen and oxides, respectively. As seen in Figure 2, the maximum potential on the spike reads $0.91 < \varphi < 0.94$ V, which corresponds to palladium oxide formation while the minimum potential on the spike reads 0.2 V. As a result, oscillations during FA on palladium have amplitude of 0.7 V, which coincides with the findings of Chen and Schell.[48] However, this amplitude is larger

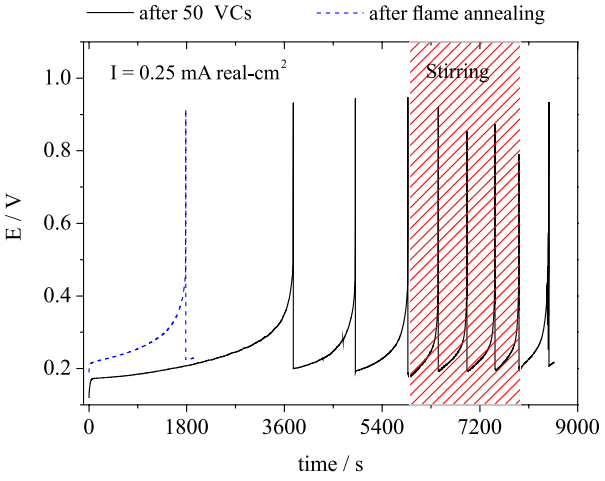

Figure 2. Temporal oscillations during formic acid electrooxidation on polycrystalline palladium (wire). Experimental conditions: chronopotentiometry measured at 1 mA; 0.1 mol L^{-1} H_2SO_4 and 0.3 mol L^{-1} HCOOH; electrochemical area: 3.88 cm^2; rugosity: 7.76.

than on platinum[24,25] that reads 0.4 or 0.3 V depending on the applied current.

The minimum potential observed during oscillations is linked with the direct FA oxidation route (path 1a). On Pd, full conversion of FA to CO_2 starts at low potential. According to Iwasita and co-workers,[16] CO_2 production during FA oxidation starts at 0.15 V and has a maximum of CO_2 production at 0.25 V. This path proceeds without production of adsorbed CO with intermediate; therefore, a fast rate of FA oxidation (path 1a) and formate decomposition (path 1b) on palladium are herein reiterated. The suppression of the indirect via (path 2a) on Pd is in agreement with a variety of other findings, for instance: adsorbed CO_{ads} is the poison resulting from FA adsorption on Pt monocrystals,[56] while on palladium, formate oxidises without detectable surface IR signal of CO.[17] Additionally, after adsorbing FA on Pd and Pt nanoparticles, a stripping was conducted, and it turns out that a peak due to oxidative CO removal is absent for Pd while it exists for Pt.[57]

As far the oscillatory regime is settled, the potential oscillates with a period of 20 min, which is very short compared with platinum, in which periods are ca. 4 s (0.07 min) or 100 s (1.66 min).[33] This difference implicates that FA poison is accumulated on the surface with a lower rate on palladium than on platinum. Roughly speaking, the suppression of the indirect via (path 2a) may account for the lower rate of CO accumulation on Pd.

Reduction of the oscillation period by half, i.e., 8.5 min, occurs with stirring the electrolyte. The shortened gradient distance for diffusion attained with stirring promotes an increase on the rate of CO_2 extraction from the surface and on the rate of FA supply to surface. As a result, concentration of FA and CO_2 in front of the electrode is increased and decreased, respectively. However, only the increased rate of FA adsorption is addressed as a mandatory process responsible for shortening the oscillatory period, i.e., increasing FA concentration in front of the electrode speeds up subsequent poisoning surface steps, presumably path 2a. The hypothesis of suppressing path 3a by stirring, due to decreased interfacial CO_2 concentration, is dismissed since an enlargement on the period, instead of a shortening, would be expected. In this concern, the effect of stirring observed herein is substantially different from that observed by Tian and Conway[23] in regard to one-point-six-maximum-amplitude galvanostatic oscillations, whose stirring electrolyte affects the permanence at the maximum potential of the spike. Presumably, those differences are linked with different oscillatory mechanisms operating on the experiments herein (0.9 V maximum potential) and on the Tian-and-Conway experiments (1.6 V maximum potential).

However, other two aspects of FA oscillatory dynamics exist, whose clarification came with the experiments shown below. The first aspect concerns a variance of the maximum oscillating potential with the stirring solution, and the shortening induction period observed with flame annealed electrode.

CO electrooxidation on static Pd electrode under continuous CO bubbling

Figure 3 shows CO electrooxidation on Pd electrode at rest, under continuous CO bubbling. On sulfate-based support electrolyte, the onset of palladium oxide formation occurs at ca. 0.7 V; however, the onset for CO oxidation occurs at ca. 0.9 V on Pd under continuous CO poisoning. At 0.9 V, CO is removed from the surface by the Langmuir-Hinshelwood mechanism, which is the so-called ignition potential. This information is useful to understand two aspects regarding the maximum potential of the oscillations seen in Figure 2.

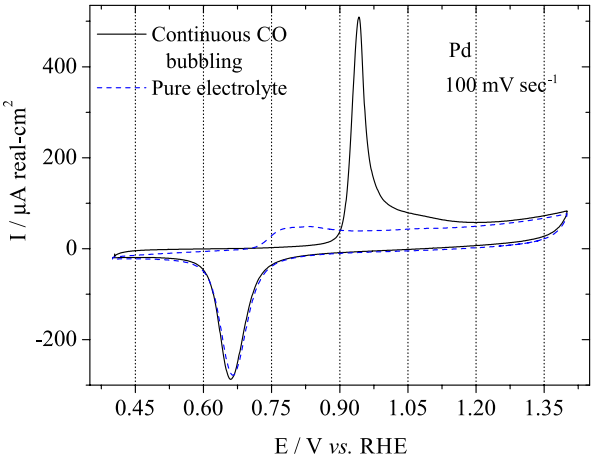

Figure 3. Continuous CO electrooxidation on palladium; continuous CO bubbling. Experimental conditions: 0.1 mol L^{-1} H_2SO_4; Pd electrochemical area: 1.89 cm^2; rugosity: 1.4.

Firstly, the maximum potential of oscillation observed in Figure 2, ca. 0.9 V *vs.* RHE, coincides with the ignition potential for continuous CO oxidation on palladium, as seen in Figure 3. This is strong evidence that carbon monoxide is still assigned as the main poisoning intermediate for the oscillating mechanism.

Secondly, slight irregularity on the maximum potential of oscillation under stirring the solution is observed in Figure 2. The four cycles observed under stirring, in Figure 2, show maximum potential of oscillation at 0.91, 0.85, 0.87 and 0.79 V *vs.* RHE. Differently from the experiments shown in Figure 3, where surface is saturated by CO since the early potentials, the rise of potential

during oscillation occurs with a progressive poison accumulation on the surface and a considerable number of remaining free sites. When the rising potential during oscillation reaches potential of ca. 0.7 V, oxides start to accumulate on the surface, and they co-exist with a high CO coverage, but forming isolated islands. The co-existence of adsorbed carbon monoxide and palladium oxide is allowed from 0.7 V till the ignition potential at ca. 0.9 V. Under perturbation (solution stirring), CO oxidation in an oscillatory state may occur at potentials lower than the ignition potential, but still in the range of potential where Pd oxide and adsorbed CO co-exist, i.e., from 0.75 to 0.9 V.

Effects of subsurface hydrogen on FA electrooxidation

Figure 4 shows cyclic voltammograms during FA electrooxidation on Pd electrodes submitted to specific conditions: (*i*) electrode flame annealed and cycled several times between 0.4 and 1.4 V (*vs.* RHE) in the presence of formic acid, and (*ii*) electrode flame annealed and immediately used in FA electrooxidation experiment. The major difference between these electrodes is the amount of hydrogen inserted into the electrode bulk. The heat treatment by flame-annealing allows hydrogen dissolved into Pd bulk attain sufficient kinetic energy to escape from the crystalline Pd lattice. Thus, this electrode is regarded as hydrogen-free. On the other hand, the treated-with-several-cycles electrode gets the opportunity to absorb hydrogen that is generated during FA electrooxidation in positive and negative potential sweep scan; and the number of moles of absorbed hydrogen increase over the number of potential cycles. We are dealing with hydrogen-free electrodes and occluded hydrogen electrodes, respectively.

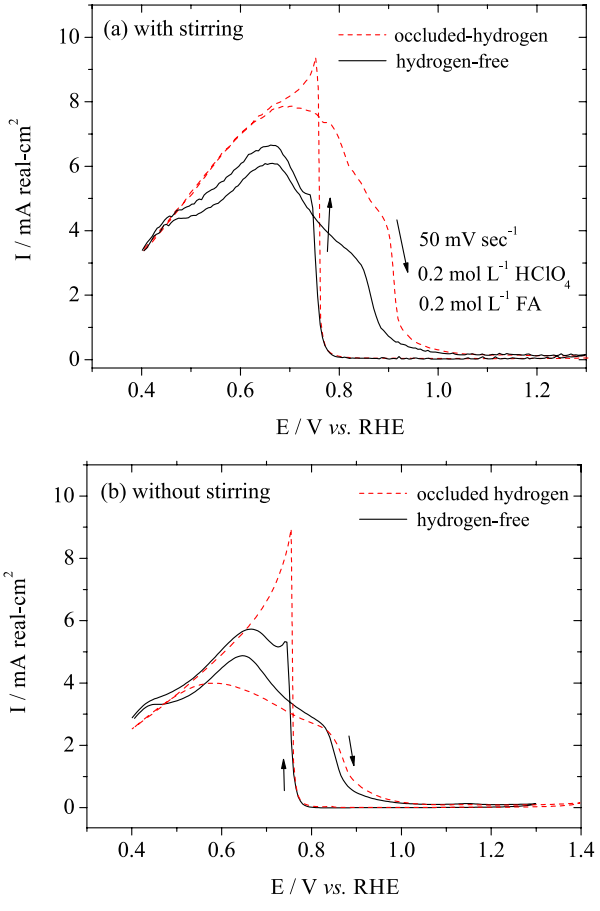

Figure 4. Cyclic voltammetry during FA electrooxidation on palladium (a) with stirring, and (b) without stirring; electrode cycled several times between 0.4 and 1.4 V in the presence of FA is regarded as an inserted-hydrogen electrode, and heat treating electrode by flame annealing is regarded as a hydrogen-free electrode. Experimental conditions: 50 mV sec^{-1}; 0.2 mol L^{-1} $HClO_4$ and 0.2 mol L^{-1} HCOOH.

Remarkably, under stirring the solution, occluded-hydrogen electrode oxidises FA with larger current than hydrogen-free electrode (Figure 4a). Under solution stirring, decreasing diffusion layer is attained; FA concentration in front of the electrode is raised; so does the current, cf. the same electrode in Figures 4a and 4b. However, this effect is much more effective on the occluded hydrogen electrode. Subsurface hydrogen presumably may have some electronic effect on its site by turning it favourable to FA adsorption and subsequent intermediates. Presumably, the thermodynamically-favourable solubility of hydrogen in the palladium bulk adds an additional driving force for dehydrogenation and/or dehydration processes. Following this hypothesis, both dehydrogenation (path 1a) and dehydration (path 2a) pathways would be accelerated with the subsurface hydrogen.

Regressing to Figure 2, the enlarged induction period found on occluded hydrogen electrodes (60 min) in comparison with hydrogen-free electrodes (30 min) may be discussed. The enlargement reflects a lower CO accumulation rate on hydrogen-free surface. According to the currently acceptable FA mechanism on Pd (Scheme 1), adsorbed CO may derive from path 3a (readsorbed CO_2) or path 2a (FA dehydration). In the paragraph above, a hypothesis for accelerated dehydration (path 2a) with subsurface hydrogen was raised; however this hypothesis is not sufficient to explain the enlarged induction period observed in Figure 2 because the faster path 2a is, the faster the rate of CO accumulation; thus, a shorter induction period would be expected while, in fact, a enlarged induction period is seen on the occluded hydrogen surface. At this point, it is not possible to dismiss some electronic effect promoted by subsurface hydrogen on the adsorption of CO_2; it is hypothesised that subsurface hydrogen deactivates the electrochemical site to adsorb CO_2. The subsurface hydrogen prevents the accumulation of adsorbed carbon monoxide derived from re-adsorption of CO_2.

The second point to be clarified in Figure 2 concerns the decreasing period of oscillation with stirring. As that observation was done for the occluded hydrogen electrode, CO accumulation is majorly driven by path 2a since the subsurface hydrogen tends to block CO_2 adsorption, as hypothesised above, while accelerating path 2a. Yépez and Scharifker[46] report a temporal decay on the higher current during formate electrooxidation on occluded-hydrogen palladium; this fact was attributed to regime limited by hydrogen diffusion into the electrode bulk.

Discussion

Oscillating mechanism

The mechanism classified as an HNDR oscillator[54] requires two characteristics: (*i*) the presence of positive and negative feedback loops, which resemble the competition in the activator-inhibitor mechanism (or prey-predator mechanism shown in the Lotka-Volterra equation), and (*ii*) a parallel reaction with large current, which is called the main current.

Formic acid electrooxidation mechanism fits properly in the requirements cited above. After adsorption, FA may follow two routes until its complete oxidation to CO_2. The indirect via shown in Scheme 1 includes CO as a strong adsorbed intermediate. The formation (path 2a) and electrooxidation (path 2b) of carbon monoxide represent a sub-network that provides the existence of positive and negative feedback loops.[58] There is a quite intuitive explanation with the help of Scheme 2 to understand this pair of loops. This network diagram displays only essential variables for an HNDR oscillation: adsorbed CO and OH. Let us start from path 2a. After FA gets adsorbed, FA dehydration produces adsorbed CO that occupies one free site. Over time, the free site total number is decreased ($\Delta* < 0$) while population of adsorbed CO is increased ($\Delta CO_{ads} > 0$); however, the electrochemical cell operates under control of a device known as galvanostat, which may be set to control the current of the WE automatically. So, a decreasing free site number promotes a decreasing current ($\Delta I < 0$), which provokes the galvanostat to react by increasing the applied potential between CE and WE which, in turn, drives the double layer voltage to higher positions ($\Delta\varphi > 0$); at higher electrode potential, FA oxidation by the indirect via gets faster and more adsorbed CO is formed, thus closing the loop ($\Delta CO_{ads} > 0$), which is mathematically translated below:

$$\frac{\Delta CO_{ads}}{\Delta *}\frac{\Delta *}{\Delta I}\frac{\Delta I}{\Delta \varphi}\frac{\Delta \varphi}{\Delta CO_{ads}} = \frac{\Delta CO_{ads}}{\Delta CO_{ads}} \quad (3)$$

Analysing the sign of all variations we discover that CO accumulation on the electrode surface belongs to a positive loop.

$$\frac{+}{-}\frac{-}{-}\frac{-}{+}\frac{+}{+} = \frac{\Delta CO_{ads}}{\Delta CO_{ads}} = \frac{+}{+} \quad (4)$$

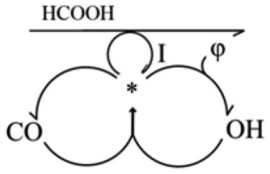

Scheme 2. Network diagram of FA electrooxidation mechanism. The asterisk represents free sites, CO and OH represent adsorbed species; I denotes the main current carried out by the loop involved with direct HCOOH electrooxidation; a straight line over this loop indicates a process with high turnover rate. Reactants and products are not shown, but only strongly adsorbed intermediates.

Let us analyse path 2a, which is a sort of Langmuir-Hinshelwood (LH) mechanism. For aqueous electrolyte, oxide formation on palladium starts at double layer voltage of 0.75 V, and the oxide is continuously accumulated on the surface at higher potential, thus forming a potential-dependent isotherm. We have learned in the positive feedback loop that electrode potential increases over time due to CO accumulation, and as soon as it reaches the potential of oxide formation, palladium oxide starts to accumulate on the surface ($\Delta OH_{ads} > 0$); however, OH_{ads} reacts with CO_{ads} through LH mechanism, and two free sites are realised while CO_2 is desorbed. The increasing total free site number ($\Delta* > 0$) leads to an increased current ($\Delta I > 0$) that is registered by the galvanostat which, in turn, reacts by decreasing the potential applied between WE and CE. The double layer voltage, thus, is decreased ($\Delta\varphi < 0$) and recovers the value at the cycle onset where no CO or OH exist, but solely free sites ($\Delta OH_{ads} < 0$); then, the loop is closed. Analysing the sign of all variations we discover that OH accumulation on the electrode surface belongs to a negative loop.

$$\frac{\Delta OH_{ads}}{\Delta *}\frac{\Delta *}{\Delta I}\frac{\Delta I}{\Delta \varphi}\frac{\Delta \varphi}{\Delta OH_{ads}} = \frac{+}{+}\frac{+}{+}\frac{+}{-}\frac{-}{-} = \frac{\Delta OH_{ads}}{\Delta OH_{ads}} = \frac{+}{-} \quad (5)$$

On the other hand, the direct via shown in Scheme 1 includes formate as an intermediate species; however, its coverage is rather low given that, as proposed by Miyake *et al.*,[20] formate is a short-lived reactive intermediate, which implicates in a situation where as soon formate is formed, it is self-decomposed to CO_2. This route represents a loop over the free sites: FA adsorption makes the total number of free sites decrease,

FA oxidises to formate, and formate is decomposed to CO_2 that desorbs and makes the total number of free sites be restored, thus closing the loop. Thus, direct path for FA electrooxidation (Scheme 1) is represented in the network diagram (Scheme 2) as a loop that is ascribed to the entire direct route rather than a specific adsorbate (formate). The straight line over this loop represents the entire direct route that now is labelled as main current because it represents a process with high turnover rate. Moreover, adsorbed formate cannot be regarded as a species that competes for the same site with other species such as CO since adsorbed formate can be replaced by CO at low potential. Formate is rather a spectator-species of the free site total number. The entire direct via shown in Scheme 1 is a spectator process with respect to the oscillating CO and OH coverages.

In brief, variances of FA mechanism kinetics on palladium in comparison with platinum indicated a suppression of indirect path (path 2a), formation of side products such as bicarbonate (path 3b), and admission of a new path, the CO_2 re-adsorption (path 3a). To complicate even more this scenario, we found that subsurface hydrogen (palladium crystalline net is a reservoir for hydrogen) assists the kinetics of CO accumulation, which were hypothesised to derive from the fact that subsurface hydrogen presumably promotes electronic effect on its site by making it favourable to adsorb FA but not to adsorb CO_2. Following this hypothesis, the kinetics of both dehydrogenation (path 1a) and dehydration (path 2a) pathways would be accelerated with the subsurface hydrogen while subsurface hydrogen deactivates the electrochemical site to adsorb CO_2. Regardless of all those variations found on Pd surface, the oscillating mechanism still remains similar to the one on platinum. Adsorbed CO is still the major poison, which is further supported by the work of Zhang *et al.*,[59] and the two antithetical feedback loops associated with the Langmuir-Hinshelwood mechanism of CO electroxidation were described above.

To conclude this discussion, the core argument to defend the resemblance between Pd and Pt concerning the oscillating mechanism of FA electroxidation derives from the morphology of oscillations shown in Figure 2. Globally, only single period was observed. Regardless of subsurface hydrogen acting by blocking electrochemical site to CO_2 adsorption, no mix mode oscillations (MMOs) were observed; but, if it were the case, subsurface would be considered as a dynamical variable with respect to the mathematical model, which, in turn, would add an extra degree of freedom to the mathematical model. As a result, an additional loop over the free sites on Scheme 2 would be required.

Other considerations

Finally, the findings described herein are somewhat dissimilar from previous ones observed by Conway and co-workers,[22,23] who observed, in addition to what was observed in Figure 2, oscillations with amplitude located between 1.4 and 1.6 V. The authors justified the appearance of high potential as a result of highly oxidised palladium (Pd^{4+}), i.e., PdO_2. Despite lacking oscillations between 1.4 to 1.6 V as observed herein, those oscillations were observed in a practical fuel cell[3] whose electrode used a mixture of Pd/C with PtRu/C as anode catalyst.

Conclusions

Two bifurcations were experimentally recognised in complex FA electrooxidation: saddle-node bifurcations (bistability) and Hopf bifurcations (oscillations). Bistability appears at relatively high values of current for an electrochemical cell controlled by a galvanostat device. The active state is represented by the surface at 0.2 V where FA is oxidised by the direct via. The inactive state is represented by a surface at 1.6 V where the surface is covered by oxide of high degree of oxidation, i.e., PdO_2. On the other hand, galvanostatic oscillations appear, but at low current.

Galvanostatic oscillations during FA electrooxidation on palladium exhibit one of the longest period observed in electrochemistry (ca. 17 min) and with one of longest induction period (ca. 60 min). Herein, a palladium foil was used as work electrode, storing a considerate amount of hydrogen into its crystalline bulk, which occurs continuously during the FA electrooxidation processes. A reduction by half of both oscillation period (ca. 8.5 min) and induction period (ca. 30 min) were observed for palladium rich in occluded hydrogen. Thus, occluded hydrogen assists the formation and accumulation of the poisoning intermediate which is ascribed to adsorbed carbon monoxide, and is also supported by the fact that the maximum potential of oscillation (ca. 0.9 V *vs.* RHE) coincided with the ignition potential observed during CO oxidation under continuous CO poisoning. The roles of subsurface (or occluded) hydrogen have been hypothesised on the basis of electronic effect caused on its electrochemical site by making it favourable to adsorb FA but not CO_2.

Despite mechanistic variations observed on Pd in comparison with Pt, FA electroxidation surface still has similar oscillating mechanism on both surfaces, i.e., oscillating Langmuir-Hinshelwood mechanism derived from the CO electrooxidation, while the dehydrogenation

path (path 1a) is considered as a parallel reaction responsible for a highly positive impedance. This argument is firstly defended by the fact that the morphology of oscillations is invariant with respect to the amount of occluded hydrogen in the electrode bulk; indicating that no additional degrees of freedom are added to the description of the dynamical model by subsurface hydrogen; secondly, the almost one-third of an hour required to accumulate adsorbed CO until the critical coverage during a single cycle of oscillation reflects the miserably low kinetics of FA dehydration (indirect pathway) and the low kinetics of CO_2 re-adsorption.

In addition to what is observed for the electrode containing subsurface hydrogen, amplitude and morphology of oscillations are also invariant with respect to solution stirring. Formic acid/formate diffusion from the electrolyte bulk toward the electrode surface and hydrogen diffusion from the electrode bulk toward subsurface positions must be disregarded as dynamic variables. Both diffusion processes are rather parameters with respect to the dynamic model that describes complex electrooxidation of formic acid.

Acknowledgements

This study was supported by CAPES (PDEE/1270/10-9), CNPQ (142739/2007-3).

References

1. Mota, A.; Eiswirth, M.; Gonzalez, E. R.; *J. Phys. Chem. C* **2013**, *117*, 12495.
2. Mota, A.; Gonzalez, E. R.; *ECS Trans.* **2013**, *58*, 1879.
3. Gonzalez, E.; Mota-Lima, A. In *Direct Alcohol Fuel Cells*; Corti, H. R.; Gonzalez, E. R., eds.; Springer: Dordrecht, Netherlands, 2014, ch. 2.
4. Mota, A.; *Kinetic Instabilities during Electroxidation of CO-containing Hydrogen: Three-Electrode Cells and Fuel Cells*, 1st ed. LAP LAMBERT Academic Publishing: Saarbrücken, Germany, 2013.
5. Parsons, R.; *Handbook of Electrochemical Constants*; Butterworths Publications: London, UK, 1959.
6. Shao, M.; *J. Power Sources* **2011**, *196*, 2433.
7. Fernandez-Vega, A.; Feliu, J. M.; Aldaz, A.; Clavilier, J.; *J. Electroanal. Chem. Interfacial Electrochem.* **1991**, *305*, 229.
8. Llorca, M. J.; Herrero, E.; Feliu, J. M.; Aldaz, A.; *J. Electroanal. Chem.* **1994**, *373*, 217.
9. Herrero, E.; Llorca, M. J.; Feliu, J. M.; Aldaz, A.; *J. Electroanal. Chem.* **1995**, *383*, 145.
10. Zhang, M.; Wilde, C. P.; *J. Electroanal. Chem.* **1995**, *390*, 59.
11. Seland, F.; Tunold, R.; Harrington, D. A.; *Electrochim. Acta* **2008**, *53*, 6851.
12. Batista, B. C.; Varela, H.; *J. Phys. Chem. C* **2010**, *114*, 18494.
13. Samjeské, G.; Miki, A.; Osawa, M.; *J. Phys. Chem. C* **2007**, *111*, 15074.
14. Clavilier, J.; Parsons, R.; Durand, R.; Lamy, C.; Leger, J. M.; *J. Electroanal. Chem. Interfacial Electrochem.* **1981**, *124*, 321.
15. Iwasita, T.; Xia, X.; Herrero, E.; Liess, H.-D.; *Langmuir* **1996**, *12*, 4260.
16. Solis, V.; Iwasita, T.; Pavese, A.; Vielstich, W.; *J. Electroanal. Chem. Interfacial Electrochem.* **1988**, *255*, 155.
17. Nishimura, K.; Kunimatsu, K.; Machida, K.-I.; Enyo, M.; *J. Electroanal. Chem. Interfacial Electrochem.* **1989**, *260*, 181.
18. Pavese, A.; Solís, V.; *J. Electroanal. Chem. Interfacial Electrochem.* **1991**, *301*, 117.
19. Pavese, A. G.; Solis, V. M.; Giordano, M. C.; *Electrochim. Acta* **1987**, *32*, 1213.
20. Miyake, H.; Okada, T.; Samjeske, G.; Osawa, M.; *Phys. Chem. Chem. Phys.* **2008**, *10*, 3662.
21. Wolter, O.; Willsau, J.; Heitbaum, J.; *J. Electrochem. Soc.* **1985**, *132*, 1635.
22. Wojtowicz, J.; Marincic, N.; Conway, B. E.; *J. Chem. Phys.* **1968**, *48*, 4333.
23. Tian, M.; Conway, B. E.; *J. Electroanal. Chem.* **2005**, *581*, 176.
24. Okamoto, H.; *Electrochim. Acta* **1992**, *37*, 37.
25. Nagao, R.; Epstein, I. R.; Gonzalez, E. R.; Varela, H.; *J. Phys. Chem. A* **2008**, *112*, 4617.
26. Angelucci, C. A.; Varela, H.; Herrero, E.; Feliu, J. M.; *J. Phys. Chem. C* **2009**, *113*, 18835.
27. Schell, M.; Albahadily, F. N.; Safar, J.; Xu, Y.; *J. Phys. Chem.* **1989**, *93*, 4806.
28. Raspel, F.; Nichols, R. J.; Kolb, D. M.; *J. Electroanal. Chem. Interfacial Electrochem.* **1990**, *286*, 279.
29. Albahadily, F. N.; Schell, M.; *J. Electroanal. Chem. Interfacial Electrochem.* **1991**, *308*, 151.
30. Schell, M.; Albahadily, F. N.; Safar, J.; *J. Electroanal. Chem.* **1993**, *353*, 303.
31. Strasser, P.; Lübke, M.; Raspel, F.; Eiswirth, M.; Ertl, G.; *J. Phys. Chem.* **1997**, *107*, 979.
32. Samjeské, G.; Osawa, M.; *Angew. Chem., Int. Ed.* **2005**, *44*, 5694.
33. Samjeské, G.; Miki, A.; Ye, S.; Yamakata, A.; Mukouyama, Y.; Okamoto, H.; Osawa, M.; *J. Phys. Chem. B* **2005**, *109*, 23509.
34. Naito, M.; Okamoto, H.; Tanaka, N.; *Phys. Chem. Chem. Phys.* **2000**, *2*, 1193.
35. Strasser, P.; Lübke, M.; Parmanada, P.; Eiswirth, M.; Ertl, G.; *J. Phys. Chem. B* **1998**, *102*, 3227.
36. Parsons, R.; VanderNoot, T.; *J. Electroanal. Chem.* **1988**, *257*, 9.
37. Chen, Y. X.; Ye, S.; Heinen, M.; Jusys, Z.; Osawa, M.; Behm, R. J.; *J. Phys. Chem. B* **2006**, *110*, 9534.
38. Gao, W.; Keith, J. A.; Anton, J.; Jacob, T.; *J. Am. Chem. Soc.* **2010**, *132*, 18377.

39. Arenz, M.; Stamenkovic, V.; Schmidt, T. J.; Wandelt, K.; Ross, P. N.; Markovic, N. M.; *Phys. Chem. Chem. Phys.* **2003**, *5*, 4242.
40. Arenz, M.; Stamenkovic, V.; Ross, P. N.; Markovic, N. M.; *Surf. Sci.* **2004**, *573*, 57.
41. Wang, J.-Y.; Zhang, H.-X.; Jiang, K.; Cai, W.-B.; *J. Am. Chem. Soc.* **2011**, *133*, 14876.
42. Lewis, F. A.; *The Palladium Hydrogen System*; Academic Press: London, UK, 1967.
43. Duncan, H.; Lasia, A.; *Electrochim. Acta* **2008**, *53*, 6845.
44. Gabrielli, C.; Grand, P. P.; Lasia, A.; Perrot, H.; *J. Electrochem. Soc.* **2004**, *151*, A1943.
45. Czerwiński, A.; Marassi, R.; Zamponi, S.; *J. Electroanal. Chem. Interfacial Electrochem.* **1991**, *316*, 211.
46. Yépez, O.; Scharifker, B. R.; *Int. J. Hydrogen Energy* **2002**, *27*, 99.
47. Yépez, O.; Scharifker, B. R.; *J. Appl. Electrochem.* **1999**, *29*, 1185.
48. Chen, S.; Schell, M.; *J. Electroanal. Chem.* **2001**, *504*, 78.
49. Koper, M. T. M. In *Advances in Chemical Physics*, vol. 92; Prigogine, I.; Rice, S. A., eds.; John Wiley & Sons: Hoboken, NJ, USA, 2007.
50. Rand, D. A. J.; Woods, R.; *J. Electroanal. Chem. Interfacial Electrochem.* **1971**, *31*, 29.
51. Biegler, T.; *J. Electrochem. Soc.* **1969**, *116*, 1131.
52. Biegler, T.; Rand, D. A. J.; Woods, R.; *J. Electroanal. Chem. Interfacial Electrochem.* **1971**, *29*, 269.
53. Capon, A.; Parsons, R.; *J. Electroanal. Chem. Interfacial Electrochem.* **1973**, *44*, 239.
54. Strasser, P.; Eiswirth, M.; Koper, M. T. M.; *J. Electroanal. Chem.* **1999**, *478*, 50.
55. Dall'Antonia, L. H.; Tremiliosi-Filho, G.; Jerkiewicz, G.; *J. Electroanal. Chem.* **2001**, *502*, 72.
56. Clavilier, J.; Sun, S. G.; *J. Electroanal. Chem. Interfacial Electrochem.* **1986**, *199*, 471.
57. Zhang, J.; Qiu, C.; Ma, H.; Liu, X.; *J. Phys. Chem. C* **2008**, *112*, 13970.
58. Eiswirth, M.; Bürger, J.; Strasser, P.; Ertl, G.; *J. Phys. Chem.* **1996**, *100*, 19118.
59. Zhang, H. X.; Wang, S. H.; Jiang, K.; André, T.; Cai, W. B. *J. Power Sources* **2012**, *199*, 165.

Submitted: November 4, 2013
Published online: May 6, 2014

FAPESP has sponsored the publication of this article.